

Gravitational lenses and plastic simulators

Ronald J. Adler, William C. Barber, and Mark E. Redar

Citation: *Am. J. Phys.* **63**, 536 (1995); doi: 10.1119/1.17865

View online: <http://dx.doi.org/10.1119/1.17865>

View Table of Contents: <http://ajp.aapt.org/resource/1/AJPIAS/v63/i6>

Published by the American Association of Physics Teachers

Related Articles

A demonstration condenser microphone

Phys. Teach. **50**, 508 (2012)

Dashboard Videos

Phys. Teach. **50**, 477 (2012)

Peer Assessment with Online Tools to Improve Student Modeling

Phys. Teach. **50**, 489 (2012)

Analyzing spring pendulum phenomena with a smart-phone acceleration sensor

Phys. Teach. **50**, 504 (2012)

Locating the Center of Gravity: The Dance of Normal and Frictional Forces

Phys. Teach. **50**, 456 (2012)

Additional information on Am. J. Phys.

Journal Homepage: <http://ajp.aapt.org/>

Journal Information: http://ajp.aapt.org/about/about_the_journal

Top downloads: http://ajp.aapt.org/most_downloaded

Information for Authors: <http://ajp.dickinson.edu/Contributors/contGenInfo.html>

ADVERTISEMENT



WebAssign®

The PREFERRED Online Homework Solution for Physics

Every textbook publisher agrees! Whichever physics text you're using, we have the proven online homework solution you need. WebAssign supports every major physics textbook from every major publisher.

webassign.net

Gravitational lenses and plastic simulators

Ronald J. Adler, William C. Barber, and Mark E. Redar
San Francisco State University, San Francisco, California 94132

(Received 28 March 1994; accepted 11 November 1994)

The deflection of light by a gravitational field is an important prediction of general relativity. It is thus an interesting problem to illustrate the deflection by simulating the appearance of astronomical objects as seen through a gravitational field. To do this we have constructed plastic lenses to simulate the gravitational deflection of light for three cases: a point mass, a sphere of constant density, and an isothermal gas sphere. In this paper we discuss the calculation of the deflection for any distribution of mass, the shape of general simulation lenses, and the construction of plastic simulation lenses. To illustrate the results we present photos of a grid, a dark spot, and a field of stars and galaxies seen through the lenses. The photos clearly display the distortion of images, Einstein rings and arcs, and brightness intensification. © 1995 American Association of Physics Teachers.

I. INTRODUCTION

The behavior of light has long played a central role in relativity theory.¹ One of the earliest verifications of general relativity was provided by the observation of starlight deflected by the sun,^{2,3} first obtained during the eclipse expeditions of 1919,⁴ only three years after the complete theory was first presented.⁵

During the last decades the gravitational lensing of light from quasars by more nearby galaxies has been found to be a fairly common phenomenon.⁶ Such lensing has even become a tool and has been used to measure the Hubble constant.⁷ Note that the word lensing as used here does not necessarily imply any focusing effect.

Recently gravitational lensing has also been used as a tool in the search for dark matter. Originally the existence of such nonluminous matter was inferred, e.g., from the motion of stars and gases in the outer regions of some galaxies;⁸ the orbital velocity is roughly constant as a function of distance, which appears to be consistent only with much more mass than the brightness indicates. Indeed it appears that most of the mass of some galaxies, about 0.90 to 0.99, is in dark matter. This is a critical question for cosmology since it bears upon the mass density and the ultimate fate of the universe. New evidence for dark matter in the form of small dark stars has come from so-called microlensing events: when a dark star passes between us and a visible star its gravitational field causes the visible star to brighten briefly.^{9,10} In this way a few dark stars have been tentatively observed.^{11,12} In an analogous way it may be possible to map out dark matter galactic halos by the specific way in which they distort the images of distant quasars.

A number of people have illustrated gravitational lensing using plastic simulators. Liebes¹³ discussed the shape and construction of a lens to simulate the effect of a point mass. Icke¹⁴ and Higbie¹⁵ further discussed the point mass simulator, and used it as a tool in studying gravitational lensing. Higbie¹⁶ discussed a simulator for a cylindrical mass distribution, roughly representing a galactic disk. It appears that others have constructed lenses for their own use but have not published the results.

We consider here lensing by both point masses and extended transparent objects. We discuss in detail how to calculate the deflection, the shape of the plastic simulator lenses, and the construction of the plastic lenses. The three specific cases we consider are a point mass, a constant density sphere, and an isothermal gas sphere. The constant den-

sity sphere was chosen for simplicity and also because the deflection can be obtained in an alternative way, i.e., by explicitly calculating the trajectory of a light ray in the Schwarzschild interior metric describing the constant density sphere. The isothermal gas sphere was chosen because it is a favored (albeit rough) model for dark matter galactic halos; the density is proportional to the inverse radius squared, which leads to a constant orbital velocity for objects at large distances, in agreement with observations.¹⁸ The plastic lenses show quite vividly the distortion of images, Einstein rings and arcs, and brightness intensification.

II. DEFLECTION BY A POINT MASS

The calculation of the deflection was first done by Einstein² and is discussed in most texts on general relativity.^{3,5} One obtains the equation of the trajectory as a null geodesic in the Schwarzschild metric, which represents the gravitational field exterior to a spherically symmetric body. When the distance of closest approach of the light to the body r is much larger than the geometric mass of the body $m = GM/c^2$, the trajectory is nearly a straight line, slightly deflected by the famous Einstein angle

$$\Delta = \frac{4m}{r}. \quad (1)$$

This is correct to first order in the ratio m/r . For a star like the sun it is about $4 \mu\text{rad}$ for a grazing ray, so use of the lowest order approximation is justified.

It is not difficult to obtain the exact trajectory of a light ray in the Schwarzschild metric in the form of an integral, which has a number of interesting features; e.g., there is a minimum

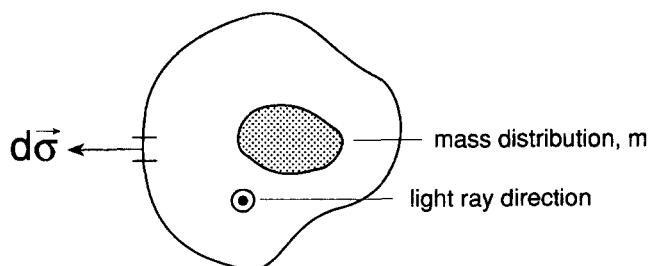


Fig. 1. The Gaussian surface is the periphery of the two-dimensional region surrounding the mass.

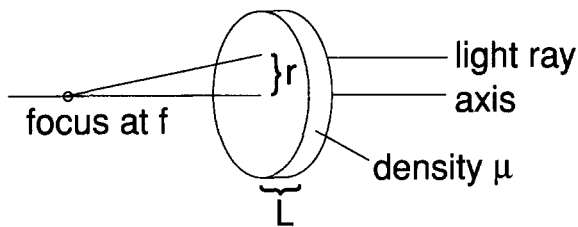


Fig. 2. Deflection by a constant density cylinder to produce focus at f .

closest approach distance. In the present paper, however, we limit ourselves to small angle deflections since a plastic lens cannot simulate large angle deflections.

III. DEFLECTION BY A MASS DISTRIBUTION: THE TWO-DIMENSIONAL ELECTROSTATIC ANALOGY

We next consider deflection by a distribution of mass, treating it as a superposition of small Einstein deflections for each particle.¹⁷ Consider a light ray passing in approximately a straight line past a group of small particles so that each particle deflects the ray towards it by the Einstein deflection. To lowest order in m/r the total deflection is a vector superposition of the individual deflections,

$$\Delta = - \sum \left(\frac{4m_i}{r_i} \right) \hat{r}_i. \quad (2)$$

Here m_i are the masses and r_i are the closest approach distances of the ray to each mass. The direction of Δ is perpendicular to the trajectory and its magnitude is the total deflection. This expression has the same form as the electrostatic field of a set of particles (with charges $q_i/4\pi\epsilon_0 = -4m_i$) in two dimensions. We may exploit the analogy to simplify the calculation for a mass distribution since Δ will obey a two-dimensional Gauss law, in analogy with Gauss' law of three-dimensional electrostatics. In the plane perpendicular to the trajectory we may write a two-dimensional Gauss' law as

$$\int \Delta \cdot d\sigma = -2\pi(4m). \quad (3)$$

Here the integral is around the region shown in Fig. 1. The vector $d\sigma$ represents the one-dimensional "surface" element of the region; its magnitude is equal to the length of the line shown, its direction is perpendicular to the line, and m is the total geometric mass inside the region. This is particularly useful for mass distributions which are radially symmetric in the plane perpendicular to the trajectory. Then Δ has constant magnitude on a circle centered on the mass distribution and points toward the center, so Eq. (3) gives for the magnitude of the deflection of a ray passing at r :

$$\Delta = \frac{4m(r)}{r} = \frac{4GM(r)}{c^2 r}. \quad (4)$$

Here $m(r)$ is the total geometric mass and $M(r)$ is the total mass inside radius r , that is within a cylinder of radius r between the light source and the observer. This expression allows easy calculation of the deflection in the cases which we will discuss here.

It is illustrative to apply Eq. (4) first to the simple case of a constant density cylinder of length L with density μ , as shown in Fig. 2.¹⁶ Then $M(r) = \pi r^2 L \mu$, and the deflection is

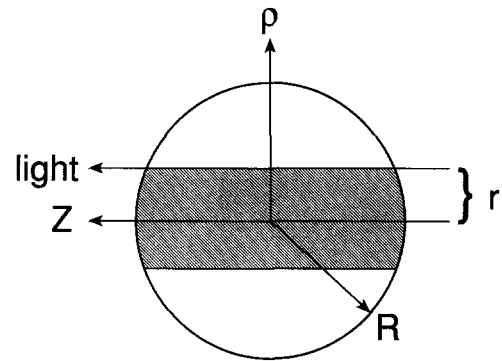


Fig. 3. Geometry of the deflection by a sphere of transparent matter. The apple-core shaped region causes the deflection.

given by

$$\Delta = \left(\frac{4\pi GL\mu}{c^2} \right) r. \quad (5)$$

That is the deflection is proportional to r , and therefore the cylinder acts as a focusing lens with focal length $f = c^2/(4\pi GL\mu)$.

IV. DEFLECTION BY CONSTANT DENSITY SPHERE

As an application of the above analysis we next consider a constant density sphere. Figure 3 shows the geometry: the sphere density is μ , its radius is R , and the light ray passes at r . Then the mass inside the region shown, an apple-core shape, contributes to the deflection according to Eq. (4). To calculate the mass we use cylindrical coordinates as shown, with ϕ being the azimuthal angle. Then

$$\begin{aligned} M(r) &= \int_{\text{core}} \mu \rho \, d\rho \, d\phi \, dz = 4\pi\mu \int_0^r \rho \, d\rho \int_0^{\sqrt{R^2-\rho^2}} dz \\ &= M \left[1 - \left(1 - \frac{r^2}{R^2} \right)^{3/2} \right], \end{aligned} \quad (6)$$

where M is the total mass of the sphere, $M = M(R) = (4\pi/3)R^3\mu$. The deflection according to Eq. (4) is thus

$$\Delta = \frac{4GM}{c^2 r} \left[1 - \left(1 - \frac{r^2}{R^2} \right)^{3/2} \right] = \frac{4m}{r} \left[1 - \left(1 - \frac{r^2}{R^2} \right)^{3/2} \right], \quad (7)$$

where m is the total geometric mass of the sphere. Note that for $r = R$ this reduces to the Einstein value, corresponding to a ray grazing the sphere. For r greater than R the deflection is given by the Einstein value in Eq. (1). Figure 4 shows Δ as a function of r . The maximum deflection occurs for $r = 0.93R$, nearly at the edge of the sphere.

We have also analyzed this problem by calculating the light ray trajectory in the interior Schwarzschild metric, which represents a constant density sphere.¹⁸ The lengthy analysis involves matching the trajectory of the light ray between the interior and exterior Schwarzschild metrics. To first order in m/r the same result, Eq. (7), is obtained, which further justifies the superposition approach.

It is interesting to study Eq. (7) for small r . To first order in r/R the deflection is

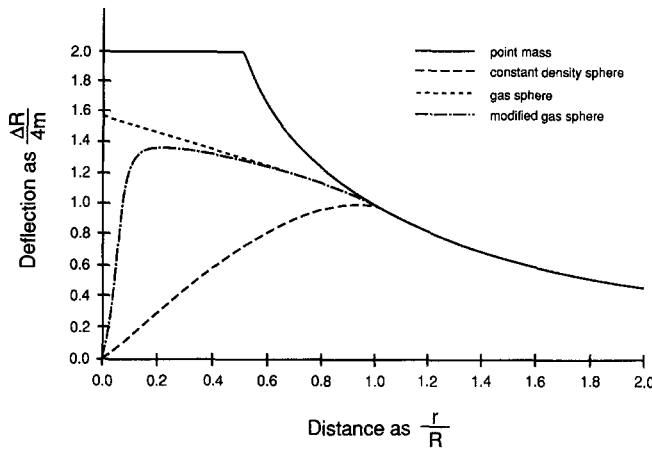


Fig. 4. Deflection caused by a point mass and various spheres. The spheres extend to $r/R=1$.

$$\Delta = \left(\frac{6m}{R^2} \right) r. \quad (8)$$

Since the deflection is proportional to r we see that the central region of the sphere acts as an approximate focusing lens, with focal length $R^2/6m$.

V. DEFLECTION BY AN ISOTHERMAL GAS SPHERE

An isothermal gas is characterized by a pressure which is proportional to its density. An isothermal gas sphere has been studied extensively, using both Newtonian theory and general relativity.^{19,20} The density is inversely proportional to the radius squared, making it a popular model for galactic dark matter halos. This implies a singularity at the origin, which we will discuss further. We restrict the gas to a sphere of radius R , with empty space outside.

The calculation of the deflection proceeds like that for the constant density sphere, except that the density μ is a function of position. In cylindrical coordinates $\mu = b/(\rho^2 + z^2)$. Using Fig. 3 we may write, as in Eq. (6), the mass inside the apple-core shaped region of radius r as

$$\begin{aligned} M(r) &= \int_{\text{core}} \mu \rho \, d\rho \, d\phi \, dz \\ &= 4\pi \int_0^r \rho \, d\rho \int_0^{\sqrt{R^2 - \rho^2}} dz \left(\frac{b}{\rho^2 + z^2} \right) \\ &= M \left[1 - \left(1 - \frac{r^2}{R^2} \right)^{1/2} + \frac{r}{R} \cos^{-1} \left(\frac{r}{R} \right) \right], \end{aligned} \quad (9)$$

where M is the total mass of the sphere, $M = 4\pi bR$. The deflection according to Eq. (4) is thus

$$\Delta = \frac{4m}{r} \left[1 - \left(1 - \frac{r^2}{R^2} \right)^{1/2} + \frac{r}{R} \cos^{-1} \left(\frac{r}{R} \right) \right], \quad (10)$$

where m is the total geometric mass of the gas sphere.

Observe that for r approaching zero the deflection (10) does not go to zero as one should expect from symmetry, but instead approaches $2\pi m/R$. This is due to the singular density at the center. Figure 4 shows the behavior of Δ as a function of r , and contrasts it with the constant density sphere.

The peculiar behavior is easily eliminated by modifying the density function to make it finite at the origin. For example, an often-used form is

$$\mu = \frac{b}{\rho^2 + z^2 + a^2} \quad (a = \text{cut-off radius parameter}). \quad (11)$$

The calculation of Δ for this density proceeds as before, and the result is

$$\Delta = \frac{4m}{r} \frac{\{1 - [1 - r^2/R^2]^{1/2} + [(r^2 + a^2)/R^2]^{1/2} \cos^{-1}[(r^2 + a^2)/(R^2 + a^2)]^{1/2} - (a/R) \cos^{-1}[a^2/(R^2 + a^2)]^{1/2}\}}{\{1 - (a/R) \cos^{-1}[a^2/(R^2 + a^2)]^{1/2}\}}. \quad (12)$$

The behavior of this expression is much like the result (10) for the unmodified gas, but for r going to zero the deflection also goes to zero. Its behavior is shown in Fig. 4 with a/R taken to be 0.02.

VI. SIMULATION LENS SHAPE: GENERAL EQUATION

We now consider how to design a plastic lens to simulate the deflection due to cylindrically symmetric mass distributions. We first examine the general problem for any $\Delta(r)$. For convenience we take the surface of the lens toward the light source to be flat and assume that the incoming rays are parallel. Most important, we limit ourselves to small deflections since large deflections cannot be simulated anyway; small angle approximations can therefore be consistently used throughout.

Figure 5 shows the geometry, with the light ray entering from the bottom and being deflected by Δ ; the thickness of the lens at r is $T(r)$ and the normal to the surface makes an angle β with the incoming ray. From the figure

$$\frac{dT}{dr} = -\tan \beta \approx -\beta. \quad (13)$$

To relate the deflection to the thickness we use Snell's law and Fig. 5 to write

$$n \sin \beta = \sin(\beta + \Delta), \quad (14)$$

where n is the refractive index of the plastic relative to air. From this we solve for β , using the small angle approximation, to obtain

$$\beta = \frac{\Delta}{n-1}. \quad (15)$$

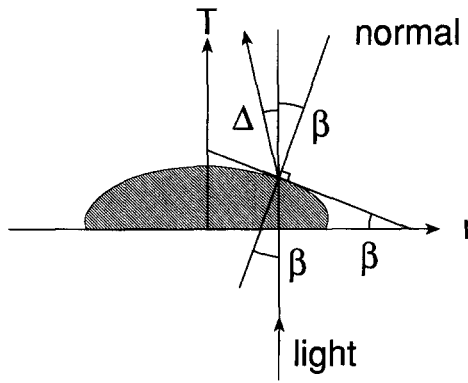


Fig. 5. Geometry of deflection by plastic lens, illustrating use of Snell's law.

Then we substitute this into Eq. (13) to obtain a differential equation for T ,

$$\frac{dT}{dr} = -\frac{\Delta(r)}{n-1}. \quad (16)$$

Note that the thickness function contains an arbitrary constant, which may be chosen for convenience.

As a simple example consider a focusing lens with focal length f . From Fig. 2 we see that the deflection function Δ is

$$\Delta \approx \tan \Delta = \frac{r}{f} \quad (\text{focusing lens}). \quad (17)$$

The lens shape is thus a parabola, a well-known result of elementary optics:

$$T = T(0) - \frac{r^2}{2f(n-1)} \quad (\text{focusing lens}). \quad (18)$$

This example corresponds to the constant mass density cylinder which we discussed in Sec. III, and for which the focal length is $f = c^2/(4\pi GL\mu)$.

VII. SIMULATION LENS SHAPES: SPECIFIC EXAMPLES

As a first application of the lens shape equation (16) we consider a point mass, for which the deflection function is given in Eq. (1). The lens shape is then logarithmic,¹³ specifically

$$T = C - \frac{4m}{n-1} \ln(r). \quad (19)$$

This diverges for small values of r , so we restrict it to r greater than some radius R . For r less than R we take the system to be opaque or to be filled with a spherical transparent mass distribution. In terms of R and $T(R)$ the thickness is

$$T = T(R) - \frac{4m}{n-1} \ln\left(\frac{r}{R}\right) \quad (\text{point mass}). \quad (20)$$

Figure 6 shows this lens shape, for $R=1$, $4m/(n-1)=1$, and $T(R)=2$.

As the second example we consider the constant density sphere of radius R , with deflection function given by Eq. (7). The integral in Eq. (16) is readily done, to give

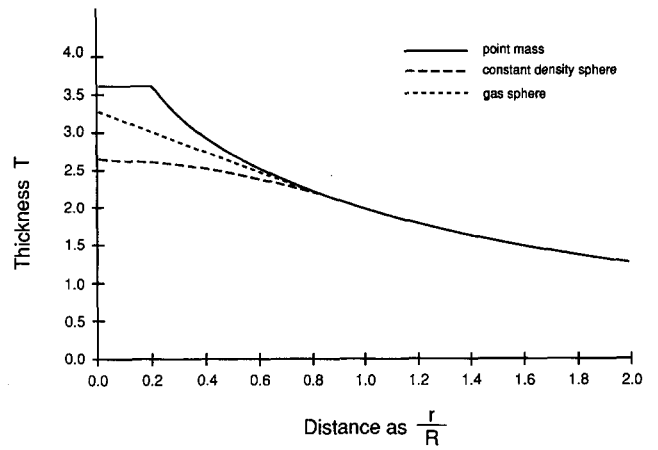


Fig. 6. Shapes of the plastic simulator lenses.

$$T = T(R) + \frac{4m}{n-1} \left\{ \frac{1}{3} \left(1 - \frac{r^2}{R^2} \right)^{3/2} + \left(1 - \frac{r^2}{R^2} \right)^{1/2} - \ln \left[1 + \left(1 - \frac{r^2}{R^2} \right)^{1/2} \right] \right\}, \quad r < R. \quad (21)$$

Notice that the deflection at $r=0$ is well behaved. For $r > R$ we use the point mass result (20) corresponding to a light ray exterior to the sphere. Figure 6 shows the lens shape, for $R=1$, $4m/(n-1)=1$, and $T(R)=2$. Note that the lens is approximately parabolic at small radius, so it will focus light incident near the center as discussed previously.

The third example is the isothermal gas sphere of radius R , with a deflection function given by Eq. (10). Integration is straightforward, and gives

$$T = T(R) + \frac{4m}{n-1} \left\{ 2 \left(1 - \frac{r^2}{R^2} \right)^{1/2} - \frac{r}{R} \cos^{-1} \left(\frac{r}{R} \right) - \ln \left[1 + \left(1 - \frac{r^2}{R^2} \right)^{1/2} \right] \right\}, \quad r < R. \quad (22)$$

For $r > R$ we again use the point mass result in Eq. (20). Figure 6 shows the shape, for $R=1$, $4m/(n-1)=1$, and $T(R)=2$. Note that the lens is conical near the center, due to

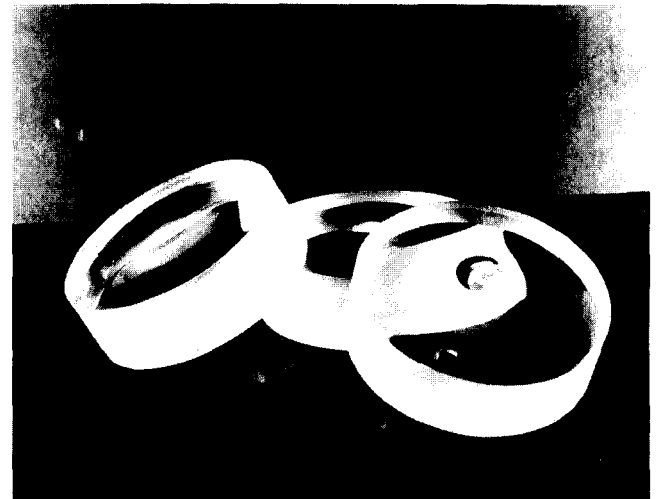
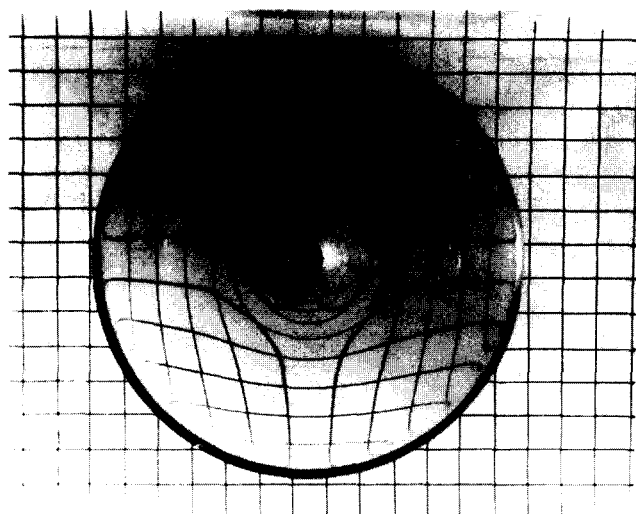
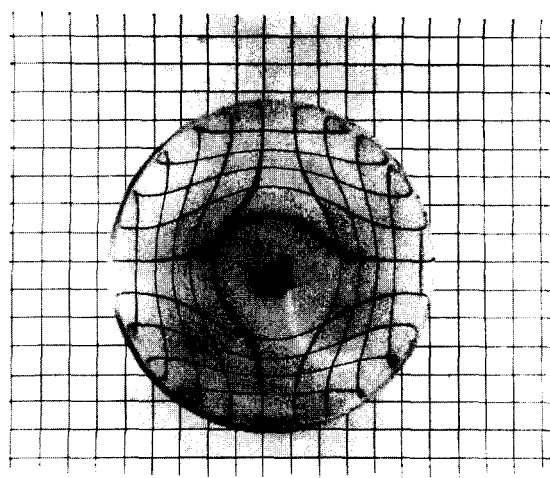


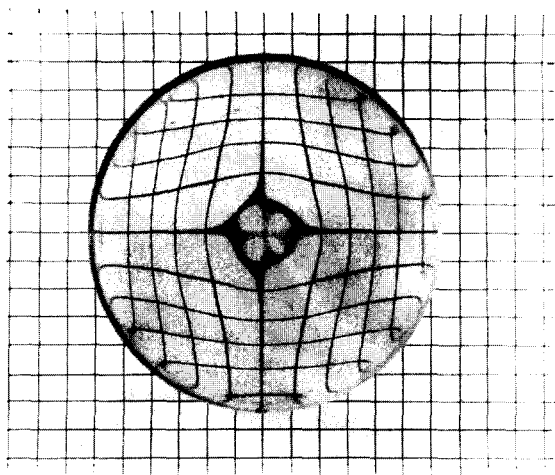
Fig. 7. Three completed plastic lenses.



(a)



(c)



(b)

Fig. 8. Square grid as seen through the lenses: (a) point mass; (b) constant density sphere; (c) isothermal gas sphere.

the singular behavior of the density at the center. However, when such a lens is constructed some degree of rounding is inevitable, so that the shape is not exactly conical; the deflection therefore corresponds to some modified density such as the one we have discussed above in Sec. V.

VIII. CONSTRUCTION OF SIMULATOR LENSES

The shape Eqs. (20), (21), or (22) of the previous section give the thickness of a simulator lens. To construct a simulator lens we began with a disk of clear plastic, about 4 in. diameter and about 1.5 in. thick. The index of refraction of plastic is about 1.5. The disk was turned on a standard metal working lathe with a 6 in. chuck, and cuts were made to give the desired thickness every 0.005 in. in the radial direction. This gave a rough step-cut lens surface, which was then smoothed on the lathe with number 600 wet emery cloth. The lens was hand smoothed and polished with toothpaste and Wright's silver polish. Figure 7 shows the three completed simulator lenses.

Since the lenses are meant to be approximate and qualitative devices the accuracy achieved with this procedure is adequate. It is clearly not necessary to grind to an accuracy

of better than a quarter wavelength as is needed for a good quality focusing lens or mirror. A computer controlled lathe would allow faster, easier, and more accurate construction. In the future we are planning to make molded lenses of plastic or epoxy.

Parameters of the three lenses were chosen for convenience in construction and not to correspond to any specific astronomical objects. For all cases we used $4m=0.0375$ in. so that $4m/(n-1)=0.075$ in. For the point mass lens we used $R=0.11$ in. and $T(R)=1.5$ in. For the constant density sphere lens we used $R=0.75$ in. and $T(0)=1.63$ in. For the isothermal gas sphere lens we used $R=1.5$ in. and $T(0)=1.5$ in.

IX. SOME IMAGES

Figure 8 shows a square grid as seen through the three lenses. The distortions of the images give clear illustrations of the lens action. Note how the grid lines are pushed outwards, and a complex pattern is produced near the center of the point mass lens.

Figure 9 shows an Einstein ring image of a dark spot as

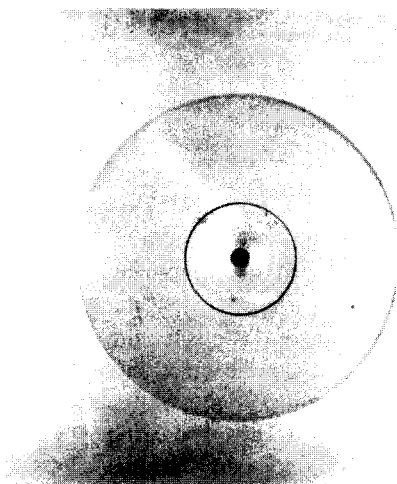


Fig. 9. Einstein ring as simulated by the point-mass lens.

seen through the point mass lens; the central dark region in the photo is the flat region of the lens and not the dark spot.

Figure 10 shows a photo containing stars and galaxies seen through the isothermal gas lens. The lens distorts galaxies, produces Einstein arcs, and intensifies some of the images. The arcs may be compared with images of real Einstein arcs in Ref. 21.



Fig. 10. Field of stars and galaxies as seen through the isothermal gas lens.

ACKNOWLEDGMENTS

We wish to thank V. Petrosian and R. Wagoner of Stanford University for discussions and references on the general problem of gravitational lensing and comments on the special cases that we have treated here. F. Drake of the University of California at Santa Cruz was helpful in discussions of previous work in constructing point-mass simulation lenses. L. Mertz was helpful in providing references and discussing his own work on simulating the effects produced by a system of many point masses.

¹A. Einstein, "Zur elektrodynamik bewegter korper," *Ann. Phys.* **17**, 891–921 (1905). An English translation is "On the electrodynamics of moving bodies," in *The Principle of Relativity* (Methuen, London, 1923) (reprinted by Dover, New York), pp. 35–65.

²A. Einstein, "Die grundlage de allgemeinen relativitatstheorie," *Ann. Phys.* **49**, 769–822 (1916). An English translation is "The foundations of the general theory of relativity," in *The Principle of Relativity* (Methuen, London, 1923) (reprinted by Dover, New York), pp. 109–164.

³R. J. Adler, M. Bazin, and M. M. Schiffer, *Introduction to General Relativity* (McGraw-Hill, New York, 1975), pp. 214–219.

⁴F. W. Dyson, A. S. Eddington, and C. Davidson, "Deflection of light by Sun's gravitational field, total eclipse of May, 1919," *Philos. Trans. R. Soc. London Sec. A* **220**, 291–333 (1920).

⁵For a summary of the eclipse measurements and more recent measurements using radio telescopes see S. Weinberg, *Gravitation and Cosmology* (Wiley, New York, 1972), pp. 188–194.

⁶For an extensive survey of the history, theory, and observations of gravitational lenses see P. Schneider, J. Ehlers, and E. E. Falco, *Gravitational Lenses* (Springer, Berlin, 1992). Known gravitational lens systems are discussed in Sec. 2.5, pp. 47–90.

⁷For a discussion of measurements of the Hubble constant see Sec. 13.1 of Ref. 6, pp. 467–476.

⁸V. Trimble, "Existence and nature of dark matter in the universe," *A. Rev. Astron. Astrophys.* **25**, 425–472 (1987).

⁹A. Einstein, "Lens-like action of a star by the deviation of light in the gravitational field," *Science* **84**, 506–507 (1936).

¹⁰See also later comments by S. Liebes, "Gravitational lenses," *Phys. Rev. B* **133**, 835–844 (1964). Reference 6 also contains a discussion of light intensification in Sec. 2.3, pp. 33–40.

¹¹C. Alcock *et al.*, "Possible gravitational microlensing of a star in the Large Magellanic Cloud," *Nature* **365**, 621–622 (1993).

¹²E. Aubourg *et al.*, "Evidence for gravitational microlensing by dark objects in the Galactic halo," *Nature* **365**, 623–625 (1993).

¹³S. Liebes, "Gravitational lens simulator," *Am. J. Phys.* **37**, 103–104 (1969).

¹⁴V. Icke, "Construction of a gravitational lens," *Am. J. Phys.* **48**, 883–885 (1980).

¹⁵J. Higbie, "Gravitational lens," *Am. J. Phys.* **49**, 652–655 (1981).

¹⁶J. Higbie, "Galactic lens," *Am. J. Phys.* **51**, 860–861 (1983).

¹⁷See Chap. 8 of Ref. 6, pp. 229–278.

¹⁸M. E. Redar, "Gravitational lenses and plastic simulators," M. S. thesis, San Francisco State University (1994).

¹⁹S. Chandrasekhar, *Introduction to the Study of Stellar Structure* (Dover, New York, 1957), pp. 84–183.

²⁰For the general relativistic problem see also Ref. 3, pp. 308–317.

²¹E. L. Turner, "Gravitational lenses," *Sci. Am.* **259**, 54–62 (1988).

DIFFERENT KINDS OF COMPLEXITY

What is really meant by the opposing terms simplicity and complexity? In what sense is Einsteinian gravitation simple while a goldfish is complex?

Murray Gell-Mann, *The Quark and the Jaguar: Adventures in the Simple and the Complex* (W. H. Freeman and Company, New York, 1994), p. 28.